Laser and Particle Beams (2003), *21*, 243–248. Printed in the USA.

DOI: 10.1017/S026303460321212X

Generation and propagation of high-current low-energy electron beams

V.N. DEVYATKOV,[1] N.N. KOVAL,[1] P.M. SCHANIN,[1] V.P. GRIGORYEV,[2] AND T.V. KOVAL[2]
[1]Institute of High Current Electronics Siberian Division of the Russian Academy of Science, Tomsk, Russia
[2]Tomsk Polytechnic University, Tomsk, Russia

(RECEIVED 1 April 2003; ACCEPTED 16 May 2003)

Abstract

High-current electron beams with a current density of up to 100 A/cm^2 generated by a plasma-cathode gas-filled diode at low accelerating voltages are studied. Two types of gas discharges are used to produce plasma in the cathode. With glow and arc discharges, beam currents of up to 150 A and 400 A, respectively, have been obtained at an accelerating voltage of 16 kV and at a pressure of $1–3\cdot10^{-2}$ Pa in the acceleration gap. The ions resulting from ionization of gas molecules by electrons of the beam neutralize the beam charge. The charge-neutralized electron beam almost without losses is transported over a distance of 30 cm in a drift channel which is in the axial magnetic field induced by Helmholtz coils. The results of calculations for the motion of electrons of the charge-neutralized beam with and without axial external field are presented and compared with those of experiments.

Keywords: Arc discharge, Electron beam; Gas-filled diode, Glow discharge; Plasma cathode

1. INTRODUCTION

Nowadays, high-current pulsed charged-particle beams with a power density of 10^6–10^8 W/cm^2 are used for surface modification of solids (Andreev *et al.*, 2000; Rotshtein *et al.*, 2000). During the interaction of the high-power beam with a surface, structural-phase transformations occur in a near-surface layer due to fast melting and cooling that causes an increase in layer microhardness and in wear resistance and a decrease in the friction coefficient. Unlike ion beams, where such power density in a thin layer obtains at ion energies of 100–300 keV (Remnev & Shulov, 1993), the electron beam ensures realization of the same processes at electron energies of no more than 40 keV. To achieve the required power density at the irradiated surface with low electron energies, high beam current densities of the order of hundreds of amperes per square centimeter are needed. In a vacuum diode, the current density, which is determined by the Child–Langmuir law, is limited by the electric strength of the acceleration gap and by high electron losses and, in some cases, by cutoff of the beam. The latter is due to radial and longitudinal potential falls produced by the space self-charge of the beam in its transportation to the site of use. The space charge, as a rule, is compensated by ions which result from ionization of the gas either by electrons of the beam or by ions of the plasma generated in the transportation channel. In the conditions of intense supply of the gas and ions into the acceleration gap and into the electron emission system, use is made of explosive-emission (Mesyats, 1998) and plasma cathodes (Koval *et al.*, 1983), which are resistant to ion bombardment and to abrupt changes in the gas pressure. Moreover, the plasma-filled and gas-filled diodes exhibit higher perveance, since the acceleration of electrons in them occurs in the space charge layer formed between the cathode and anode plasmas under definite conditions. So, with a plasma-cathode gas-filled diode based on glow and arc discharges, emission current densities of up to 100 A/cm^2 were obtained at microsecond pulse durations (Zharinov *et al.*, 1986; Devyatkov *et al.*, 2001), whereas with an explosive-emission-cathode diode, emission current densities ranged to several hundreds of amperes per square centimeter at nanosecond pulse durations (Nazarov *et al.*, 1994).

This article presents the results of the study of the generation of high-current low-energy electron beams in a plasma-cathode gas-filled diode based on glow and arc discharges. Consideration is given to the problems of transportation of high-current beams in a low-pressure gas and on simulation of this process.

Address correspondence and reprint requests to: Nikolay N. Koval, High Current Electronics Institute SD RAS, 4 Akademichesky Ave., 634055 Tomsk, Russia. E-mail: koval@opee.hcei.tsc.ru

2. GENERATION AND PROPAGATION OF ELECTRON BEAMS

Figure 1 shows schematically the design of the gas-filled diode and that of the beam transportation system. The gas-discharge system of the plasma cathode consists of two discharge systems. The first one is formed by cylindrical cathode *1* of internal diameter 10 mm and length 50 mm and by hollow anode *3* of diameter 40 mm and length 50 mm and is the initiating glow discharge system.

To decrease the glow discharge initiating voltage, the cathode is immersed in the axial magnetic field induced by permanent magnets *2*. The second system of the main discharge comprises electrode *3*, which is a hollow cathode in this system, and hollow anode *6* of diameter 88 mm and length 100 mm. Two discharge systems are coupled through constriction hole *5* of diameter 6 mm in electrode *3*. Inside electrode 3, annular magnesium insert *4* of height 10 mm can be mounted. At the face of the hollow anode there is a hole of diameter 50 mm covered with fine grid *7*. The mesh size of the grid is 0.1×0.1 mm and its transparency is 40%. The grid emission electrode is insulated from the hollow anode. For ease of switching the discharge into the emission electrode, the latter is connected to a discharge power supply. The hollow anode and the emission electrode are connected through a resistor (R1 = 100 Ω). An acceleration electrode in the form of a diaphragm which is 2 mm larger than the emission hole in diameter is located 5–8 mm from the grid. The electron beam is transported in a drift channel of diameter 52 mm and length 200 mm. The drift channel is in a uniform magnetic field of induction $B_z = 5 \cdot 10^{-3}$–$2 \cdot 10^{-2}$ T induced by two Helmholtz coils *10*. The coils are located outside the vacuum chamber and are spaced 200 mm apart. A movable Faraday cup *11* is used to diagnose the beam at a distance of 50–250 mm from the emission grid. The discharge, emission, and beam currents in the electrode circuits of the discharge system are measured by Rogowski coils. The vacuum chamber is pumped to a pressure of $p = 1 \cdot 10^{-3}$ Pa by a turbomolecular pump at a pumping rate of 1000 L/s.

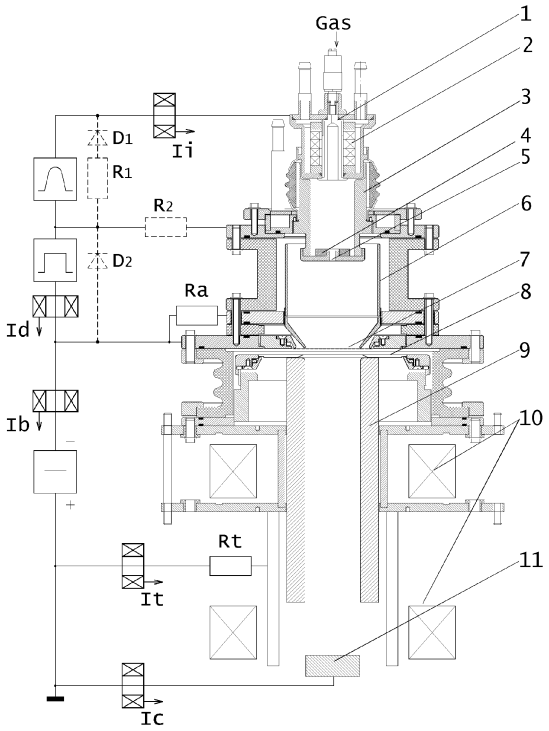

Fig. 1. Designs of the gas-filled diode and beam transportation system.

3. RESULTS OF INVESTIGATION OF GAS-FILLED DIODES

3.1. Plasma-cathode diode based on a glow discharge

In experiments, two modes of the initiation and operation of a glow discharge were used. An initiating discharge of 2–3 μs duration and current amplitude 30 A is ignited at a voltage of 5 kV and at a relatively high pressure due to a pressure drop in the constriction hole and produces the primary plasma in the hollow cathode of the main discharge. This allows a substantial decrease in operating pressure at which the main glow discharge between the hollow cathode *3* and the hollow anode 6 is ignited and operates in its high-current form (Vizir *et al.*, 1997) and an increase in the electric strength of the acceleration gap.

The main discharge between electrodes *3* and *4* is initiated with a time delay of 2–4 μs at a voltage of 900 V, whereupon it is switched to the grid electrode *5* due to limitation of the current by the resistance R1. The variations in pressure in the range from $1 \cdot 10^{-1}$ to $1 \cdot 10^{-3}$ Pa slightly affect the operating voltage of the main discharge. The introduction of diodes D1, D2, and resistor R2 connected in series into the circuit of the discharge system and the increase in the length of the constriction channel from 12 mm to 40 mm cause a change in the operating conditions of the main discharge and a considerable decrease in voltage (to 500 V). Upon cessation of the initiating discharge, a low-current (6–10 A) discharge then operates between electrodes *2* and *3*, and the operating voltage of the main discharge decreases with increasing discharge current (Fig. 2). Probe measurements have shown that with a main discharge current of 140–160 A, plasma of density $n_p = 10^{13}$ cm^3, and temperature $T_e = 7$ eV is generated in the hollow anode near the ∅10-mm grid electrode.

Electrons are extracted from the plasma through the emission grid and are accelerated by dc voltage controllable in the range from 5 kV to 20 kV. Figure 3 shows the current-voltage characteristic of the gas-filled diode. It can be seen in this figure that the diode current is nearly constant in a wide range of the accelerating voltage, and at low voltages it far exceeds the current determined by the Child–Langmuir law.

https://doi.org/10.1017/S026303460321212X Published online by Cambridge University Press

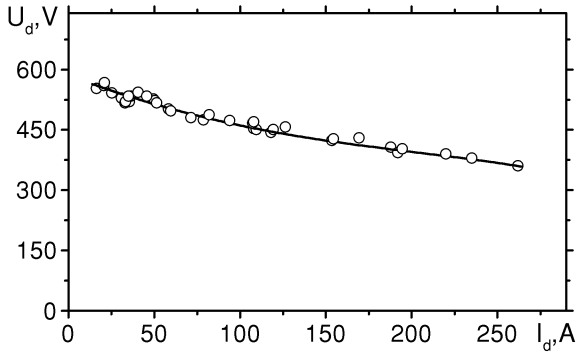

Fig. 2. Discharge voltage versus the main discharge current.

Such a character of the dependence can be explained in the following manner. The extracted electrons ionize the gas in the acceleration gap and in the drift channel and produce the anode plasma. The boundary of this plasma is at a distance from the grid anode such that it is possible to pass a plasma cathode saturation current of the density:

$$j = en[kT_e/(2\pi m)]^{1/2}, \quad (1)$$

where e is the electron charge, n is the plasma electron density, k is Boltzmann's constant, T_e is the electron temperature, and m is the electron mass.

With a discharge current of 200 A, an accelerating voltage of 15 kV, and an emission hole diameter of 10 mm, a diode current of 80 A with an accelerated electron current density of 100 A/cm^2 has been obtained. This density is an order of magnitude higher than that calculated for a separation of 5 mm between the grid electrode and the acceleration diaphragm by the Child–Langmuir law. According to the relation which determines the electron and ion current densities j_e and j_i in the layer:

$$j_e = j_i(M/m)^{1/2} = 1.85 \cdot 2.33 \cdot 10^{-6} \cdot U^{3/2}/d^2, \quad (2)$$

where M is the ion mass, U is the accelerating voltage, and d is the layer length, the layer width which provides such electron current density in experiment is no greater than 2 mm. With such a layer width, the ion current density $j_i = 3 \cdot 10^{-2}$ A/cm^2 and the anode plasma density $n_a = 4 \cdot 10^{11}$ cm^{-3}, respectively. The beam electron density $j_b = 1 \cdot 10^{11}$ cm^{-3}.

Therefore, it can be expected that the ions of the anode plasma in the drift channel will compensate the space charge of the beam, thus making possible its transportation without appreciable losses.

3.2. Plasma-cathode diode based on an arc discharge

The further increase in beam current in a diode based on a glow discharge is limited by the discharge-to-arc transition that takes place with increasing main discharge current. Hence, a plasma-cathode arc discharge is used to obtain higher beam currents. To increase the stability of the initiation of the arc, a Mg insert with a height of 40 mm and with the same internal diameter as the constriction hole is placed in the region of the constriction hole.

As in a diode based on a glow discharge, the current in the acceleration gap depends almost not at all on the accelerating voltage, when varied from 4 to 20 kV, and increases according to something like the linear law with increasing discharge current (Fig. 4). At low discharge currents, the main discharge is first ignited in the glow mode almost simultaneously with an increase in initiating discharge current and within 4–6 μs after the initiation, the discharge-to-arc transition takes place. As the discharge current is increased, the time delay decreases and levels off at 2–3 μs (Fig. 5).

Characteristic waveforms of the main discharge currents, diode currents, and collector currents for a grid electrode diameter of 50 mm and for the rated beam current are shown in Figure 6. It can be seen in this figure that the efficiency of electron extraction from the cathode plasma, α, is high and is close to unity ($\alpha = I_b/I_d$ is the ratio of the current in the acceleration gap to the discharge current), which is deter-

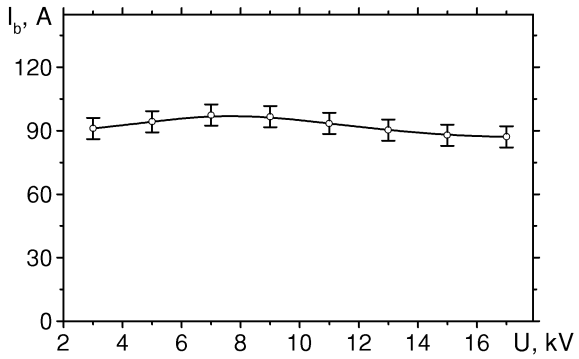

Fig. 3. Beam current versus the accelerating voltage.

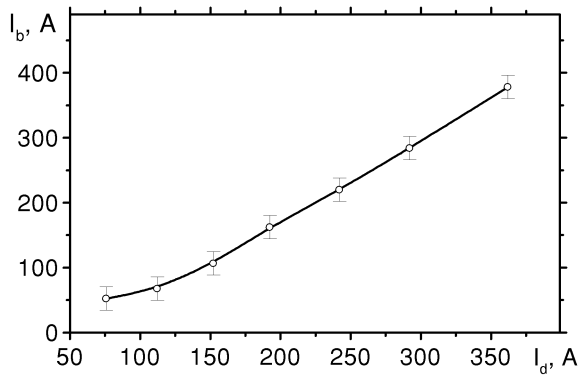

Fig. 4. Beam current I_b versus the discharge current I_d. $p = 3 \cdot 10^{-2}$ Pa, $U = 15$ kV.

https://doi.org/10.1017/S026303460321212X Published online by Cambridge University Press

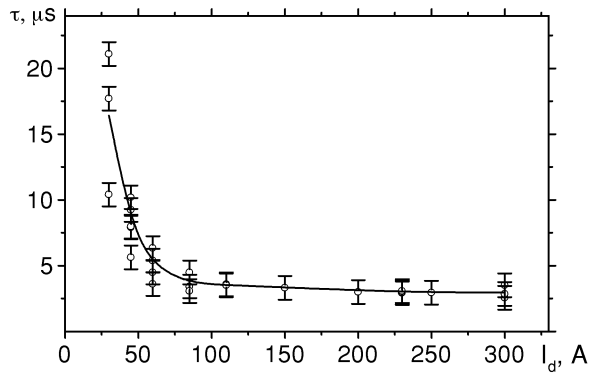

Fig. 5. Time of the glow-to-arc discharge transition versus the main discharge current.

mined by the discharge current and by the position of the anode plasma boundary in the acceleration gap.

It should be noted that the gas pressure affects both the parameters of the diode and the transportation of the beam. Decreasing the pressure causes instability of electron extraction and a substantial decrease in diode current, giving rise to high-frequency current oscillations during the pulse rise time. Such operation of the diode is mainly due to a lack of the ions resulting from ionization of the gas. In these conditions, the width of the layer between the anode plasma boundary and the grid electrode is governed by the passage of the saturation ion current according to the Child–Langmuir law. Such a width of the layer does not provide passage of the saturation ion current in the acceleration gap, and the transportation of the beam in the drift channel is made difficult by incomplete compensation of the space charge of the beam.

4. PROPAGATION OF ELECTRON BEAMS IN THE GAS

The accelerated electrons come in the drift channel and, ionizing the gas, produce plasma there. The space charge of the beam is completely neutralized in the conditions wherein the electron beam density equals the plasma ion density. The rate of change in the ion density in the drift channel is determined by the relation

$$dn_{i/}/dt = n_b \sigma_i n_g v - n_e n_i \alpha, \tag{3}$$

where n_b is the beam electron density, n_g is the gas molecule density, σ_i is the ionization cross section, v is the electron velocity, $\alpha = 10^{-25} \cdot n_i / T_e^{4.5}$ is the coefficient of recombination by an electron impact (Golant *et al.*, 1977), and $n_e = n_i - n_b$.

Without accounting for the electron losses during the beam current pulse risetime and for the recombination of plasma ions due to a low value of the coefficient α, the time it takes for complete neutralization of the space charge in the first approximation can be determined from the expression

$$\tau = 1/n_g \sigma_i v, \tag{4}$$

With the beam parameters presented in Figure 6, the estimated time is no longer than 4 μs, which agrees with experiment.

Without an external magnetic field, instabilities arise in the charge-neutralized beam because of its pinch by the magnetic self-field. These instabilities result in substantial electron losses. In particular, chaotic motion of the beam over a distance of 1–2 cm is observed at a target located 35 cm from the cathode.

The equation of motion of electrons in the axial magnetic field $B_z(z)$, which is nonuniform along the length of the drift channel, can be presented in the form

$$\ddot{x} = \frac{eB_\varphi}{m_0 r_b \beta_z \cdot \gamma}[1 - f_e - \beta_z^2(1 - f_M)]x - \frac{eB_z}{\gamma m_0 c}\dot{y} + \frac{e\beta_z}{\gamma m_0}\tilde{B}_r y, \tag{5}$$

$$\ddot{y} = \frac{eB_\varphi}{m_0 r_b B_z \cdot \gamma}[1 - f_e - \beta_z^2(1 - f_M)]y + \frac{eB_z}{\gamma m_0 c}\dot{x} - \frac{e\beta_z}{\gamma m_0}\tilde{B}_r x, \tag{6}$$

$$\ddot{z} = \frac{eB_\varphi}{m_0 r_b B_z \cdot \gamma}(\beta_x \cdot x + \beta_y \cdot y) - \frac{e}{\gamma m_0}\tilde{B}_r(\beta_x \cdot y - \beta_y \cdot x), \tag{7}$$

where $\beta_z = \dot{z}/c$, $\beta_x = \dot{x}/c$, $\beta_y = \dot{y}/c$, $\tilde{B}_r = -\frac{1}{2}dB_z/dz$, $B_\varphi = (2I)/(r_b c)$ is the magnetic field of the beam, γ is the relative electron energy, e and m_0 are the elementary charge and mass of an electron, and c is the velocity of light.

The presented system of equations makes it possible to study the motion of the electron beam in various conditions of transportation taking into account variations in the beam radius $r_b(z)$. In so doing, the degree of charge and magnetic

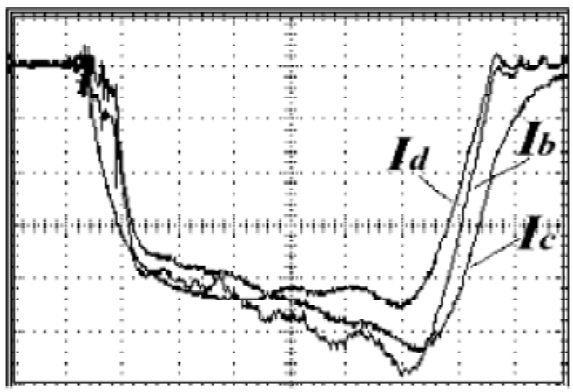

Fig. 6. Typical waveforms of the discharge current I_d, the emission current I_b, and the collector current I_c. Scale: 100A/div., time: 5 μs/div, $U = 16$ kV, $p = 2.6 \cdot 10^{-2}$ Pa, $B = 0.02$ T.

https://doi.org/10.1017/S026303460321212X Published online by Cambridge University Press

(current) neutralizations (f_e, f_M) are determined from analysis of the time of neutralization owing to ionization of the gas by the beam and to the processes induced during the beam current pulse rise time.

In the case where the external magnetic field is absent, the position of the beam crossover z_c and the beam radius r_c are determined by the expressions derived from the solution of the equations of motion of electrons in the magnetic self-field (1–3).

$$z_c = r_{b0}\frac{2k-1}{2\sqrt{2}}\left[\frac{I}{I_A}\frac{\gamma\beta_z^3}{|1-f_e-\beta_z^2(1-f_M)|}\right]^{1/2},$$

$$r_c = \left[\frac{1}{n_i \pi r_k \beta_Z}\frac{I}{I_A}\right]^{1/2}. \qquad (8)$$

Here, r_{b0} is the beam radius at the entry to the drift channel, κ is the number of a crossover, $r_k = e^2/mc^2$ is the classical electron radius, $I_A = 17\ \kappa$A is the Alfven current. Calculations show that with an initial beam radius $r_{b0} =$ 2.5 cm, the first crossover with a beam radius $r_c = 0.7$ cm is positioned inside the drift channel at a distance of about 9 cm from the cathode. Downstream of the first crossover, electron losses occur due to expansion of the beam and to the rise of its instability.

To stabilize the beam, the copper drift channel is immersed in an axial magnetic field which is in three times higher than the azimuth self-field of the beam. The axial external magnetic field prevents the beam from being pinched and the conditions of ionization of the gas and the character of the motion of electrons are thus changed, that is, the degree of modulation of the beam decreases and the bend-type instability disappears. The position of the crossover and the degree of modulation depend heavily on the beam current density at the entry to the drift channel and on the nonuniformity of the emission current density.

Figure 7 shows calculated paths of the external electron (the beam envelope) for a varying axial magnetic field. Increasing the magnetic field causes an increase in oscillation frequency and a decrease in modulation degree.

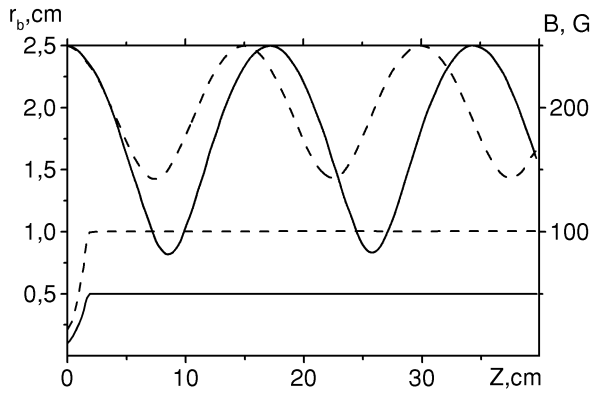

Fig. 8. Influence of the magnetic field on the paths of the external electrons. $B = 0.005$ T (solid line), $B = 0.01$ T (dashed line). $I_b = 400$ A, $U = 16$ kV.

In an actual system, there is just some transition region with increasing magnetic field, rather than the plasma cathode being fully immersed in the magnetic field. In this region, the beam is additionally pinched under the action of the radial component of the magnetic field

$$B_r = -\frac{1}{2}\frac{rdB_z}{dz}. \qquad (9)$$

In the case where the width of the transition region is small (Fig. 8), the radial magnetic field does not exert any effect on the beam, the pulsation frequency and the modulation degree just slightly increase. Increasing the width of the transition region and the magnetic field (Fig. 9) causes an increase in pulsation frequency and a decrease in modulation degree and in maximum beam radius.

The parameters of the beam upon its transportation in the drift channel were measured at a distance of 35 cm from the acceleration electrode with the Faraday cup or a calorimeter. With an accelerating voltage of 16 kV and a magnetic filed $B = 0.02$ T, a beam with a current of 400 A is transported in the drift channel without losses (Fig. 6). The increase in

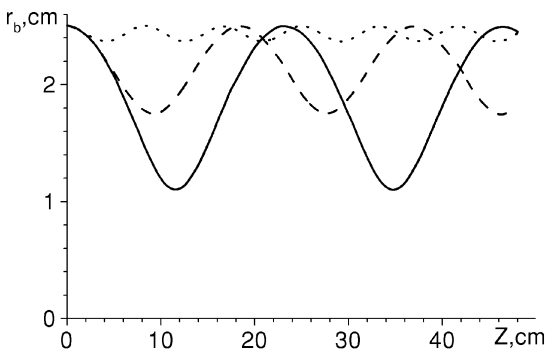

Fig. 7. Paths of the external electrons; $B = 0.005$ T (solid line), $B = 0.01$ T (dashed line), $B = 0.03$ T (doted line), $I_b = 200$ A, $U = 16$ kV.

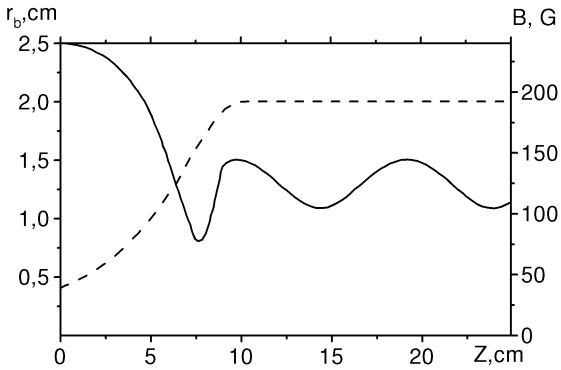

Fig. 9. Path of an external electron (solid line) for an elongated transition region of increasing magnetic field (dashed line).

https://doi.org/10.1017/S026303460321212X Published online by Cambridge University Press

diode and beam currents at the end of the pulse is presumably associated with the passage of the ion current in the acceleration gap in the first case and with the current of magnetized slow electrons from the anode plasma to the collector in the second one. With the beam diameter D = 2 cm estimated from melting of the collector (Fig. 10), the beam current density j_b is ~130 A/cm^2 and the plasma cathode emission current j_c is 20 A/cm^2.

Calorimetric measurements have shown that in the drift channel with a magnetic field, 80% of the beam energy is transferred to the collector. Calculations indicate that it is possible to ignore the beam energy losses on inelastic collisions, since over a drift length L = 30 cm and at a pressure $p = 2\cdot10^{-2}$ Pa, the losses calculated by the formula

$$\Delta E = \sqrt{2n}_p \cdot \sigma_i \cdot L \cdot I_i \tag{10}$$

are not higher than $6\cdot10^{-6}$. Here, σ_i is the ionization cross section and I_i = 15.7 eV is the ionization potential. The energy loss is most probably due to the double-beam instability arising at the frequency

$$\omega_b = \omega_p = (4\pi e^2 n_p/m)^{1/2}. \tag{11}$$

In the first approximation, these losses can be determined from the relation

$$\Delta E = \frac{2\beta^2}{3}\left(\frac{3n_b v^2}{2n_p v_T^2}\right)^{1/3} E_b, \tag{12}$$

where n_b is the electron beam density, v_T is the thermal velocity of plasma electrons, and E_b is the beam electron energy. At a plasma electron temperature of 3–4 eV, the beam loses about 22% of its energy.

4. CONCLUSION

Gas-filled diodes allow generation of electron beams of much higher perveance than that of the beams produced by vacuum diodes. The use of a plasma cathode in the diode provides a high emission density and simplifies transportation of the beam in the drift channel. This is due to the fact that in definite conditions, the beam charge is neutralized by the plasma ions resulting from ionization of the gas by the electron beam at operating pressures of $1–2\cdot10^{-2}$ Pa. At such pressures and at accelerating voltages of 15–20 kV, the acceleration gap retains sufficient electric strength. The instabilities of the charge-neutralized beam are suppressed by transportation of the beam in the cylindrical copper channel immersed in a weak (of the order of 0.02 T) axial magnetic field which is three times higher than the magnetic self-field of the beam. The beam produced has been employed in experiments on pulsed thermal treatment of materials.

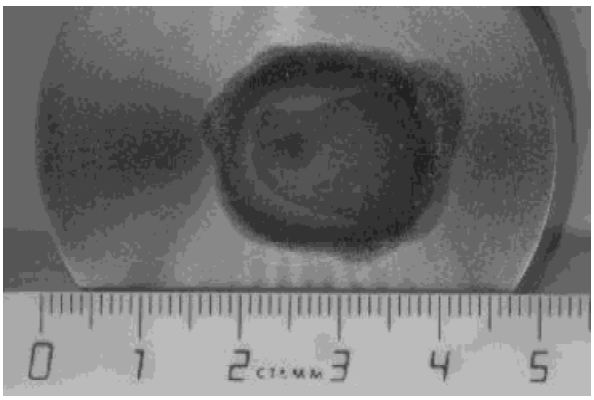

Fig. 10. Imprint of the beam on the Ti collector; $p = 2\cdot10^{-2}$ Pa, j_b = 100 A/cm^2, U = 16 kV.

REFERENCES

Andreev, A.D., Engelko, V.I., Müller, G., Nochovnay, N.A., Shulov, V.A. & Vinogradov, M.V. (2000). Electron beam technologies for surface modification and recycling of compressor and turbine blades of aircraft engines. In *Proc. 5th Conf. on Modification of Materials with Particle Beams and Plasma Flows*, pp. 245–249. (Mesyats, G., Bugaev, S. & Ryabchikov, Eds.). Tomsk, Russia: Tomsk Polytechnic University, Institute of High Current Electronics.

Devyatkov, V.N., Koval, N.N. & Schanin, P.M. (2001). Gas-filled electron diode based on a glow discharge. *Tech. Phys.* **46**, 524–528. Translated from *Sov. Phys. Tech. Phys.* 2001, **71**, 20–24.

Golant, V.E., Zhilinsky, A.P. & Sakharov, S.A. (1977). *Bases of Physics of Plasma.* Moscow: Atomisdat.

Koval, N.N., Kreindel, Yu.E. & Schanin, P.M. (1983). Generation of pulse electron beams having a uniform distribution of high current density in sources with a grid plasma emitter. *Sov. Phys. Tech. Phys.* **53**, 1846–1848.

Mesyats, G.A. (1998). *Explosive Electron Emission*. Yekaterinburg: URO-Press.

Nazarov, D.S., Ozur, G.E. & Proskurovsky, D.I. (1994). Generation of a low energy, high current beams in the gun with plasma anode. *Izvestiya Vusov. Fizika*. **3**, 100–114.

Remnev, G.E. & Shulov, V.A. (1993). Application of High-power ion beam for technology. *Laser Part. Beams* **11**, 707–709.

Rotshtein, V.P., Proskurovsky, D.I., Ozur, G.E., Ivanov, Yu.F. & Markov, A.B. (2000). Treatment of Metal and Alloys with Low-energy, High-current Electron Beams: General Characteristics, Mechanisms, Applications. In *Proc. 5th Conf. on Modification of Materials with Particle Beams and Plasma Flows*, pp. 250–257. (Mesyats, G., Bugaev, S. & Ryabchikov, Eds.). Tomsk, Russia: Tomsk Polytechnic University, Institute of High Current Electronics.

Vizir, A.V., Oks, E.M., Schanin, P.M. & Yushkov, G.Yu. (1997). Non-self-sustained hollow-cathode glow discharge for large-aperture ion sources. *Tech. Phys.* **42**, 611–614. Translated from *Sov. Phys. Tech. Phys.* **67**, 27–32.

Zharinov, A.V., Kovalenko, Yu. A., Roganov, I.S. & Tyuryukanov, P.M. (1986). Plasma emitter of electrons with a grid stabilization of emission boundary. *Sov. Phys. Tech. Phys.* **56**, 687–693.

https://doi.org/10.1017/S026303460321212X Published online by Cambridge University Press